REPORT

CIRCADIAN RHYTHMS

Structures of the cyanobacterial circadian oscillator frozen in a fully assembled state

Joost Snijder,[1]*† Jan M. Schuller,[2]*‡ Anika Wiegard,[3] Philip Lössl,[1] Nicolas Schmelling,[3] Ilka M. Axmann,[3] Jürgen M. Plitzko,[2] Friedrich Förster,[2,4]§ Albert J. R. Heck[1]§

Cyanobacteria have a robust circadian oscillator, known as the Kai system. Reconstituted from the purified protein components KaiC, KaiB, and KaiA, it can tick autonomously in the presence of adenosine 5′-triphosphate (ATP). The KaiC hexamers enter a natural 24-hour reaction cycle of autophosphorylation and assembly with KaiB and KaiA in numerous diverse forms. We describe the preparation of stoichiometrically well-defined assemblies of KaiCB and KaiCBA, as monitored by native mass spectrometry, allowing for a structural characterization by single-particle cryo–electron microscopy and mass spectrometry. Our data reveal details of the interactions between the Kai proteins and provide a structural basis to understand periodic assembly of the protein oscillator.

Many organisms, from cyanobacteria to animals, have adapted to Earth's day-night cycle with the evolution of an endogenous biological clock. These clocks enable circadian rhythms of gene expression and metabolism with a period close to 24 hours. Many circadian rhythms rely on complex networks of transcription-translation feedback, but simpler posttranslational oscillations have also been described in both cyanobacteria and human red blood cells (*1*). The circadian oscillator of cyanobacteria is composed of three components: the proteins KaiC, KaiB, and KaiA (*2*). This posttranslational oscillator is robust enough to allow reconstitution simply through incubation of purified recombinant KaiC, KaiB, and KaiA in the presence of adenosine 5′-triphosphate (ATP) (*3*). The in vitro oscillator can maintain a stable rhythm for weeks (*4*, *5*), allowing for its detailed study.

The proteins of the Kai system collectively generate a circadian rhythm based on assembly dynamics associated with KaiC autophosphorylation and dephosphorylation (*6*, *7*). KaiC forms a homohexamer consisting of two stacked rings of domains CI and CII, which have adenosine 5′-triphosphatase (ATPase) and kinase activity, respectively (*8*). During the subjective day, the kinase activity of KaiC is stimulated by the binding of KaiA to the intrinsically disordered C-terminal regions of KaiC, resulting in sequential autophosphorylation at Thr^{432} and Ser^{431} of KaiC (*9*). During the subjective night, KaiB interacts with phosphorylated KaiC, forming the KaiCB complex (*8*). Binding of KaiB to KaiC changes the activities of SasA and CikA, which are key signaling proteins of clock-output pathways that modulate transcription (*10*). Moreover, the KaiCB complex exposes an additional KaiA-binding site, sequestering KaiA and thus preventing its productive association with KaiC (*11*). The sequestration of KaiA allows KaiC to readopt its default autodephosphorylation activity, thereby slowly resetting the protein clock to an unphosphorylated state (*4*).

Atomic-level structures of the individual Kai proteins are available (*12*–*14*), but structural information on the KaiCB and KaiCBA complexes is still ambiguous (*15*–*18*). KaiB forms monomers, dimers, and tetramers in solution, with six KaiB monomers binding cooperatively to one KaiC hexamer (*19*). It has been unclear whether KaiB binds to the CI or CII domain of KaiC (*11*, *15*, *19*–*21*). Nuclear magnetic resonance (NMR) spectroscopy studies of engineered and truncated Kai proteins suggested that KaiB binds the KaiC-CI domain and only one subunit of a KaiA dimer (*11*), but it is unclear whether the wild-type, full-length proteins arrange similarly in the KaiCBA complex. Here we use mass spectrometry (MS) and cryo–electron microscopy (cryo-EM) to study the assembly and structures of the full-length clock components to provide a structural basis for the assembly dynamics of the in vitro circadian oscillator.

The standard in vitro Kai oscillator consists of a 2:2:1 molar ratio of KaiC:KaiB:KaiA in the presence of excess MgATP, incubated at 30°C (*3*). We tracked the phosphorylation-dependent assembly of the Kai proteins under these conditions and used native MS to determine the masses and stoichiometries of the formed noncovalent assemblies (*22*). For the in vitro Kai oscillator, we simultaneously detected multiple co-occurring Kai-protein complexes, revealing more than 10 different Kai protein–assembly stoichiometries over the course of 24 hours (Fig. 1A and table S1).

The KaiC starting material had low amounts of phosphorylation. Upon initial mixing, most KaiC therefore existed as a free hexamer, whereas a small fraction formed a complex with one or two KaiA dimers (fig. S1A). These KaiCA complexes have autophosphorylation activity, which led to cooperative formation of phosphorylated $KaiC_6B_6$ complexes through a $KaiC_6B_1$ intermediate (*19*). In our samples, formation of KaiCA and KaiCB complexes peaked at 4 to 8 hours incubation time. The formation of higher-order KaiCBA complexes followed the formation of KaiCB complexes, with a maximum at 8 to 12 hours of incubation followed by a steady decline toward 24 hours. We observed $KaiC_6B_6$ with between one and six KaiA dimers bound. Detailed assignments of peaks and repeated measurements are shown in Fig. 1B and figs. S1 to S3. During the dephosphorylation phase (16 to 24 hours), as KaiCBA complexes disassemble, we detected $KaiA_2B_1$ complexes in the lower-mass region of the spectra (fig. S1B). Thus, the disassembly pathway of the KaiCBA complexes appears not to be simply the reverse of the assembly pathway but rather a distinct route.

We attempted to freeze Kai-protein assembly in specific states, producing particles amenable to more detailed structural characterization. Whereas at 30°C the default activity of KaiC is autodephosphorylation, autophosphorylation is favored at 4°C (*7*, *17*). Therefore, we tested how a lower incubation temperature affected assembly of the complete in vitro oscillator. At 4°C, KaiCBA-complex formation was slower than at 30°C. However, KaiCBA abundance steadily increased, and, even after 24 hours, it did not peak (Fig. 1A). This indicated a possible route for preparation of KaiCBA complexes with full occupancy of the KaiA-binding site. Therefore, we incubated KaiC, KaiB, and KaiA at a 1:3:3 molar ratio at 4°C for one week in the presence of MgATP. We observed near-complete occupancy of the KaiA-binding site, as seen from the predominant formation of $KaiC_6B_6A_{12}$ assemblies (Fig. 1C). The measured mass of this complex was 823.3 ± 0.5 (standard deviation) kDa, compared to a theoretical mass of 821.3 kDa for $KaiC_6B_6A_{12}$ (table S1). Similarly, prolonged incubation of KaiC with KaiB at 4°C resulted in the efficient formation of $KaiC_6B_6$ complexes (measured: 426.9 ± 0.1 kDa; theoretical: 426.4 kDa; table S1). Further experiments revealed that formation of the KaiCB complex is the limiting step for the complete assembly of KaiCBA (fig. S1C).

[1]Biomolecular Mass Spectrometry and Proteomics and Netherlands Proteomics Center, Bijvoet Center for Biomolecular Research, and Utrecht Institute for Pharmaceutical Sciences, Utrecht University, Padualaan 8, 3584 CH, Utrecht, Netherlands. [2]Max Planck Institute of Biochemistry, Department of Molecular Structural Biology, D-82152 Martinsried, Germany. [3]Institute for Synthetic Microbiology, Cluster of Excellence on Plant Sciences (CEPLAS), Heinrich Heine University Düsseldorf, D-40225 Düsseldorf, Germany. [4]Cryo-electron Microscopy, Bijvoet Center for Biomolecular Research, Utrecht University, Padualaan 8, 3584 CH, Utrecht, Netherlands.
*These authors contributed equally to this work. †Present address: Department of Biochemistry, University of Washington, Seattle, WA 98195, USA. ‡Present address: Max Planck Institute of Biochemistry, Department of Structural Cell Biology, D-82152 Martinsried, Germany.
§Corresponding author. Email: a.j.r.heck@uu.nl (A.J.R.H.); f.g.forster@uu.nl (F.F.)

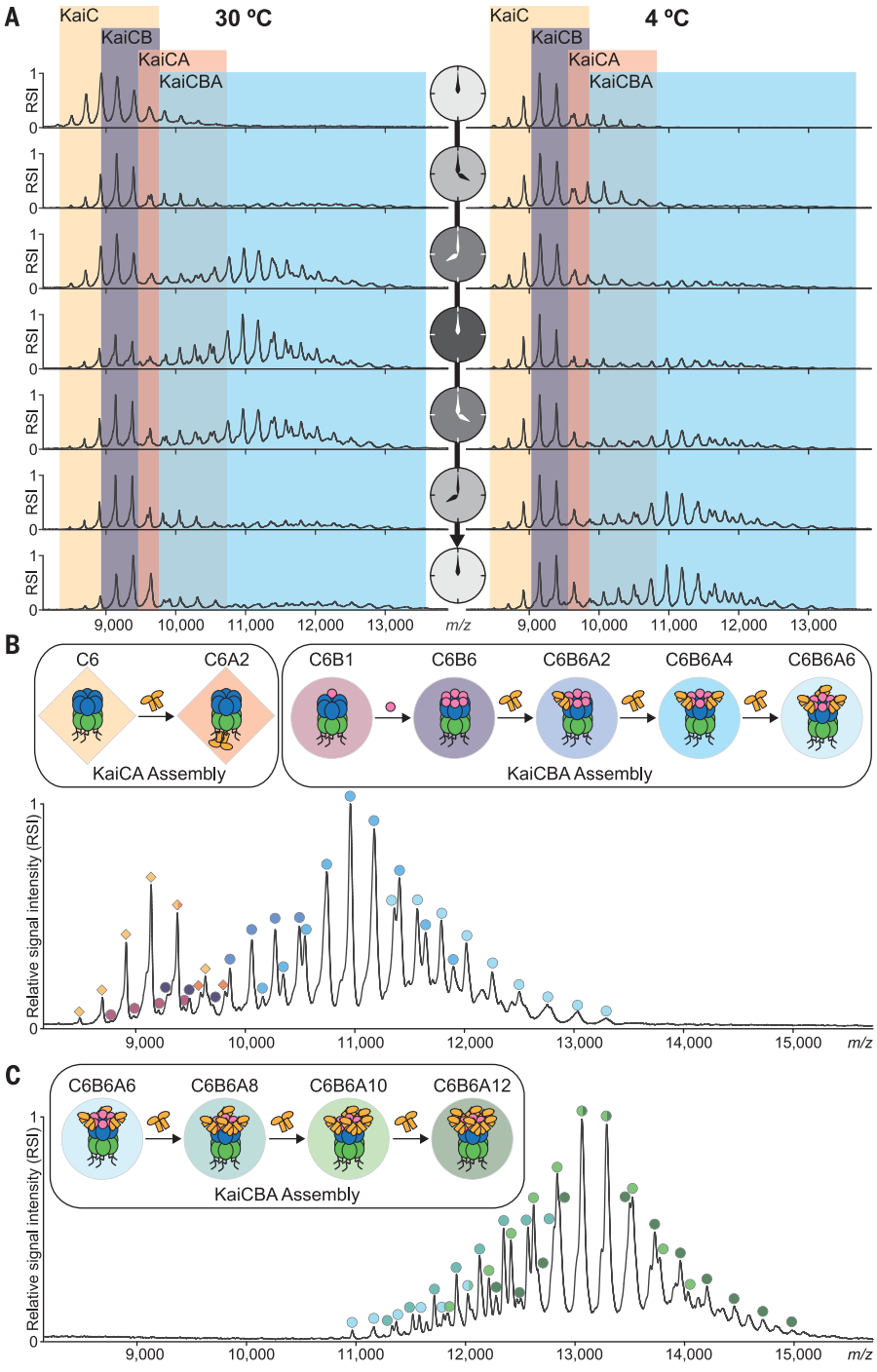

Fig. 1. Monitoring KaiCBA assembly dynamics by native MS. (**A**) Native mass spectra of the in vitro oscillator at 30° or 4°C, as indicated. The relative signal intensity (RSI) is plotted against the mass-to-charge ratio (*m/z*). Areas of the spectra corresponding to KaiC, KaiCA, KaiCB, and KaiCBA are indicated. (**B** and **C**) Enlarged mass spectra with full peak annotation. The identified Kai complexes are schematically represented above the spectra (KaiC-CI, green; KaiC-CII, blue; KaiA, yellow; KaiB, pink). The complexes are highlighted with differently colored circles and diamonds that match the symbols used to label the mass spectrum. A detailed explanation of the peak assignment is provided in fig. S2. An overview of all mass assignments is given in table S1. (B) Mass spectra of oscillator at 30°C after 12 hours of incubation. (C) Mixture of KaiCBA containing excess KaiA and KaiB incubated for 1 week at 4°C. These Kai complexes have near-complete occupancy of the KaiA-binding site.

Using the protocol described above, we obtained near-homogeneous $KaiC_6B_6A_{12}$ and $KaiC_6B_6$ assemblies, which we further structurally characterized by single-particle cryo-EM (Fig. 2). Preferred orientations of particles in ice limited the overall resolution of the KaiCB reconstruction to 7 Å, whereas the KaiCBA map was resolved to 4.7 Å (figs. S4 and S5). Superposition of the KaiCB and KaiCBA maps indicated that the KaiCB subcomplex remained essentially invariant in the KaiCBA complex (fig. S4). Both maps clearly show that KaiB binds to the KaiC-CI domain, resolving a controversy in the field (*11*, *19*–*22*). This architecture was further confirmed by cross-linking MS experiments (fig. S6 and table S2). For a molecular interpretation of the cryo-EM maps, we fitted available atomic models of their constituents (Fig. 2C).

The KaiCB structure is composed of three stacked rings (Fig. 2). Fitting of the homohexameric KaiC crystal structure (*12*) showed that the bottom two rings correspond to KaiC, and the upper ring is accordingly assigned to KaiB. A comparison of the map to the various nucleotide-bound states of the KaiC-CI domain indicated that this domain is in an adenosine 5′-diphosphate (ADP)–bound state (fig. S7) (*23*). The nucleotide-binding sites at the CI domain showed an unaccounted for density, which was hence assigned to a bound nucleotide (Fig. 2D).

The KaiB subunits are arranged in a six-fold symmetrical ring, stacked on the lids of the small KaiC-CI–ATPase subdomains (fig. S8). Isolated KaiB of the cyanobacterium *Synechococcus elongatus* exists in two different folds (*24*). One fold, seen only in KaiB to date, has been observed in protein crystals (*14*, *15*, *25*, *26*). NMR spectroscopy experiments suggested that KaiB switches from the fold observed in crystal structures to a thioredoxin-like fold upon binding to KaiC (*24*). The cryo-EM map of KaiCBA confirmed that KaiC-bound KaiB adopts the thioredoxin-like fold (fig. S9). The observed KaiC-KaiB interface is further supported by hydrogen-deuterium exchange (HDX)–MS experiments (fig. S8, table S3, and data files S1 to S3). The KaiCBA model predicted that KaiC-Ala^{108} is an essential part of the KaiC-KaiB interface. Indeed, by native MS we observed loss of binding upon mutation of Ala^{108} (fig. S10). The position of individual KaiB subunits in the KaiCBA model also suggests possible KaiB-KaiB contacts that could promote cooperativity of KaiB binding to KaiC (fig. S11).

The KaiA protein from *S. elongatus* is composed of an N-terminal pseudoreceiver (PsR) domain and a C-terminal α-helical domain that takes part in homodimerization (*13*). KaiA dimerization is consistent with the $KaiC_6B_6A_{12}$ stoichiometry determined for the fully assembled complex. Fitting of the KaiA dimer structure into the KaiCBA map (Fig. 2) yields excellent colocalization of secondary-structure elements in the map and the model for the C-terminal dimerization domain and is further supported by HDX-MS experiments (fig. S12). KaiB binds to KaiA most prominently with its β_2 strand, which is present in both KaiB folds and comprises the evolutionarily most-conserved residues of the protein (fig. S13). The KaiCBA model predicts that KaiB-Lys^{42}

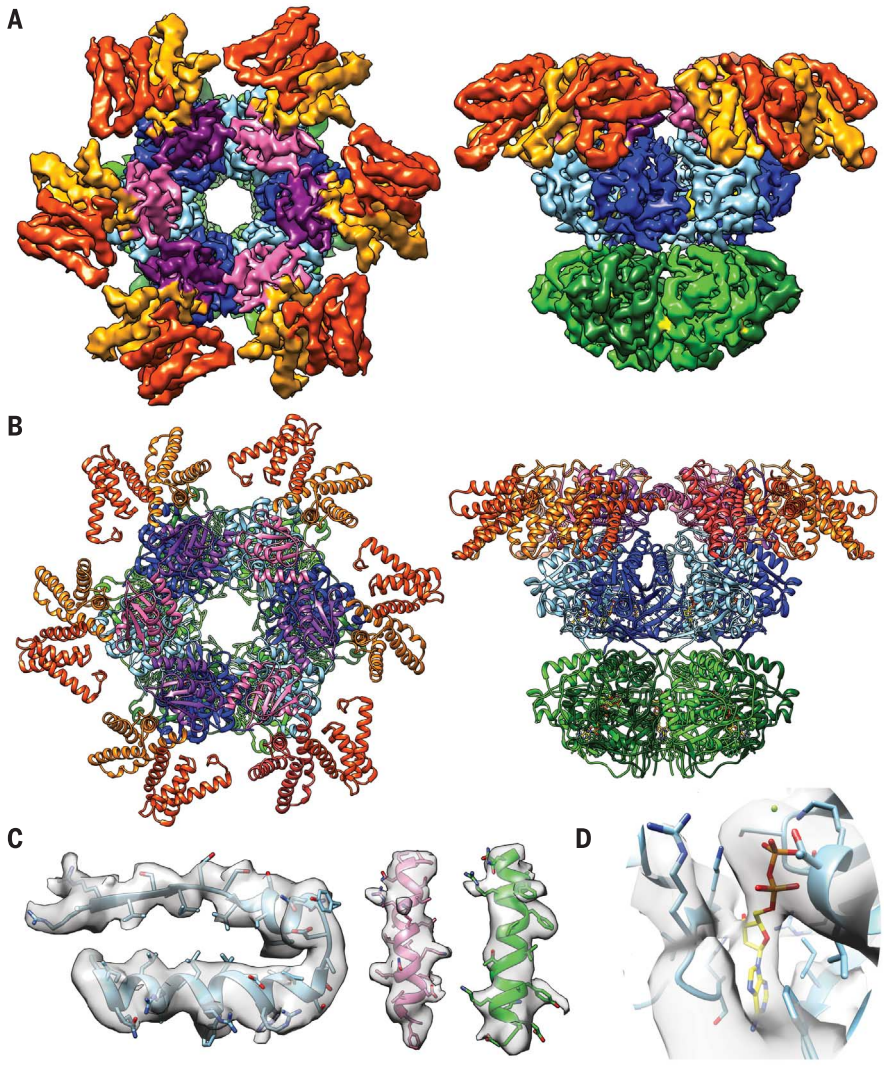

Fig. 2. Cryo-EM map and pseudoatomic model of the KaiCBA complex. (**A**) Top and side view of the three-dimensional (3D) reconstruction of the KaiCBA complex. The CII and CI domains of KaiC are colored in dark green and green and in blue and light blue, respectively. The segmented density corresponding to KaiB is colored alternating in pink and purple, and the individual KaiA homodimers are colored orange and orange-red. (**B**) Top and side view of the model of the KaiCBA complex. Colors are the same as in (A). (**C**) Selected examples of the quality of the map. (**D**) Density in the nucleotide-binding pocket of the KaiC-CI domain superimposed with the nucleotide bound in the KaiC crystal structure bound to ADP (Protein Data Bank 4TLA chain C).

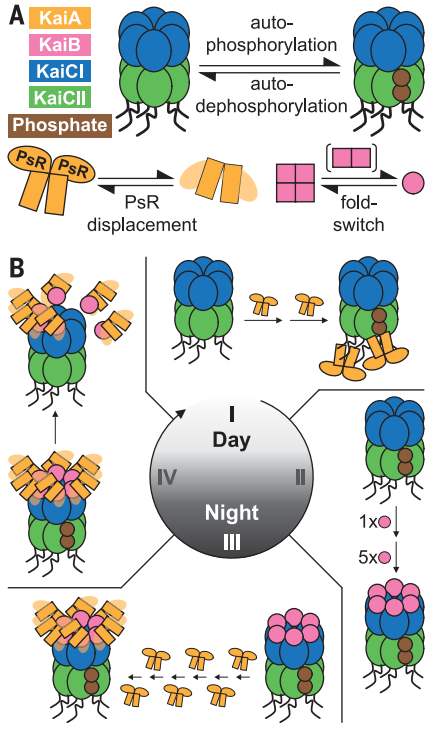

Fig. 3. The structural basis of periodic assembly in the cyanobacterial circadian clock. (**A**) Structural transitions of the individual Kai proteins during the circadian cycle. (**B**) Molecular changes in the KaiCBA oscillator. Stepwise binding of two KaiA dimers triggers KaiC autophosphorylation at Thr^{432} and Ser^{431} (I). These phosphorylation events enable cooperative binding of fold-switched KaiB monomers to the KaiC-CI domain, forming the KaiCB complex (II). KaiCB provides a scaffold for the successive sequestration of KaiA in ternary KaiCBA assemblies, concurring with a rearrangement of the KaiA PsR domains (III). KaiA sequestration promotes KaiC autodephosphorylation, resulting in the regeneration of free KaiC through release of KaiBA subcomplexes (IV).

is important for the KaiB-KaiA interaction, which was confirmed by loss of KaiA binding upon mutation of KaiB at this site, as observed in native MS experiments (fig. S10). The presence of KaiB-Lys^{42} is also important for the in vivo clock in *S. elongatus* and *Thermosynechococcus*, as *kaiBC* and *psbA* promotor activities become arrhythmic upon mutation of this site (*25*).

For every KaiA dimer in the KaiCBA model, only one monomer is in contact with KaiB. The HDX-MS data also showed signs of asymmetric binding, confirming that the two KaiA protomers in the dimer are distinct in the KaiCBA complex (fig. S14). The density assigned to KaiA in the KaiCBA map does not cover most of the N-terminal PsR domain, indicative of the domain's structural flexibility. Positioning of the PsR domains according to the fitted domain-swapped crystal structure also results in extensive clashes with KaiB (fig. S15). HDX-MS experiments do not indicate that the PsR domain unfolds or becomes disordered (table S3 and data file S1). We therefore suspect that the PsR domain is still folded, but attached with a flexible linker, which would explain the lack of density in the cryo-EM map of the KaiCBA complex. We did observe a small, unassigned KaiA-density segment near the cleft between the homodimeric C-terminal domains. We tentatively assigned this segment to residues 147 to 172, which form the small cross-β sheet and the N-terminal α5 helix in the KaiA crystal structure (fig. S15). Binding of KaiB to the linker region of KaiA therefore appears to dissociate the two strands in the dimer, resulting in a large displacement of the PsR domain. The α5 helix of KaiA likely occludes the site to which the flexible C termini of KaiC bind (*27*).

On the basis of these structures and our native MS data, we propose a detailed model for the cyclic phosphorylation-dependent assembly of Kai components in the in vitro oscillator (Fig. 3). Upon mixing the protein components of the in vitro oscillator, unphosphorylated KaiC hexamers bind one or two copies of a KaiA dimer on the C terminus of the KaiC-CII domain (*9*). Binding of the second KaiA dimer stimulates autophosphorylation of KaiC, first at Thr^{432} and then at Ser^{431} (*7*). Serine phosphorylation triggers binding of KaiB in a fold-switched state. Six copies of KaiB bind cooperatively (*19*) to form phosphorylated $KaiC_6B_6$ complexes. The bound KaiB subunits present alternative binding sites for KaiA, away from a phosphorylation-stimulating interaction with the KaiC-CII domain. The KaiA dimer binds

asymmetrically through its linker region to KaiB, resulting in a wide displacement of the PsR domain. As the pool of free KaiA dimers is depleted, KaiC switches back to autodephosphorylation activity. Complete dephosphorylation of KaiC results in dissociation of the KaiCBA complex by loss of $KaiA_2B_1$ subcomplexes, thereby completing one cycle of the oscillator. In cyanobacterial cells, KaiC and KaiB are produced from the same operon and in 10- to 100-fold excess to KaiA (*28*). The high excess of KaiCB over free KaiA could promote efficient sequestration of KaiA in vivo. The model presented here can thus serve as a framework to better understand the circadian clock in cyanobacterial cells.

REFERENCES AND NOTES

1. J. S. O'Neill, A. B. Reddy, *Nature* **469**, 498–503 (2011).
2. M. Ishiura *et al.*, *Science* **281**, 1519–1523 (1998).
3. M. Nakajima *et al.*, *Science* **308**, 414–415 (2005).
4. C. Brettschneider *et al.*, *Mol. Syst. Biol.* **6**, 389 (2010).
5. H. Ito *et al.*, *Nat. Struct. Mol. Biol.* **14**, 1084–1088 (2007).
6. M. Egli, C. H. Johnson, *Curr. Opin. Neurobiol.* **23**, 732–740 (2013).
7. T. Nishiwaki *et al.*, *EMBO J.* **26**, 4029–4037 (2007).
8. X. Qin *et al.*, *Proc. Natl. Acad. Sci. U.S.A.* **107**, 14805–14810 (2010).
9. R. Pattanayek *et al.*, *EMBO J.* **25**, 2017–2028 (2006).
10. J. S. Markson, J. R. Piechura, A. M. Puszynska, E. K. O'Shea, *Cell* **155**, 1396–1408 (2013).
11. R. Tseng *et al.*, *J. Mol. Biol.* **426**, 389–402 (2014).
12. R. Pattanayek *et al.*, *Mol. Cell* **15**, 375–388 (2004).
13. S. Ye, I. Vakonakis, T. R. Ioerger, A. C. LiWang, J. C. Sacchettini, *J. Biol. Chem.* **279**, 20511–20518 (2004).
14. R. Murakami *et al.*, *J. Biol. Chem.* **287**, 29506–29515 (2012).
15. S. A. Villarreal *et al.*, *J. Mol. Biol.* **425**, 3311–3324 (2013).
16. S. Akiyama, A. Nohara, K. Ito, Y. Maéda, *Mol. Cell* **29**, 703–716 (2008).
17. R. Pattanayek *et al.*, *PLOS ONE* **6**, e23697 (2011).
18. M. Egli, *J. Biol. Chem.* **289**, 21267–21275 (2014).
19. J. Snijder *et al.*, *Proc. Natl. Acad. Sci. U.S.A.* **111**, 1379–1384 (2014).
20. R. Pattanayek *et al.*, *EMBO J.* **27**, 1767–1778 (2008).
21. Y. G. Chang, R. Tseng, N. W. Kuo, A. LiWang, *Proc. Natl. Acad. Sci. U.S.A.* **109**, 16847–16851 (2012).
22. J. Snijder, A. J. Heck, *Annu. Rev. Anal. Chem. (Palo Alto Calif.)* **7**, 43–64 (2014).
23. J. Abe *et al.*, *Science* **349**, 312–316 (2015).
24. Y. G. Chang *et al.*, *Science* **349**, 324–328 (2015).
25. R. Iwase *et al.*, *J. Biol. Chem.* **280**, 43141–43149 (2005).
26. K. Hitomi, T. Oyama, S. Han, A. S. Arvai, E. D. Getzoff, *J. Biol. Chem.* **280**, 19127–19135 (2005).
27. R. Pattanayek, M. Egli, *Biochemistry* **54**, 4575–4578 (2015).
28. Y. Kitayama, H. Iwasaki, T. Nishiwaki, T. Kondo, *EMBO J.* **22**, 2127–2134 (2003).

ACKNOWLEDGMENTS

We thank J. Andres and M. Yazdanyar for help with protein expression, O. Mihalache for help with sample preparation, F. Beck and A. Aufderheide for assistance with image processing, and C. Benda for help with PHENIX software. This work was supported by the Netherlands Organisation for Scientific Research (NWO) Roadmap Initiative Proteins@Work grant 184.032.201 to A.J.R.H., the European Union Seventh Framework Programme ManiFold grant 317371 to A.J.R.H. and P.L., and the German Research Foundation grant GRK1721 to F.F., and grants AX 84/1-3 and EXC 1028 to A.W., N.S., and I.M.A.

SUPPLEMENTARY MATERIALS

www.sciencemag.org/content/355/6330/1181/suppl/DC1
Materials and Methods
Figs. S1 to S15
Tables S1 to S4
References (*29*–*51*)
Data S1 to S3

10 June 2016; accepted 13 February 2017
10.1126/science.aag3218

Editor's Summary

Molecular clockwork from cyanobacteria

The cyanobacterial circadian clock oscillator can be reconstituted in a test tube from just three proteins––KaiA, KaiB, and KaiC––and adenosine triphosphate (ATP). Tseng *et al.* studied crystal and nuclear magnetic resonance structures of complexes of the oscillator proteins and their signaling output proteins and tested the in vivo effects of structure-based mutants. Large conformational changes in KaiB and ATP hydrolysis by KaiC are coordinated with binding to output protein, which couples signaling and the day-night transitions of the clock. Snijder *et al.* provide complementary analysis of the oscillator proteins by mass spectrometry and cryo–electron microscopy. Their results help to explain the structural basis for the dynamic assembly of the oscillator complexes.

Science, this issue p. 1174, p. 1181